ARTICLE

Energy Analysis of a Real Industrial Building: Model Development, Calibration via Genetic Algorithm and Monitored Data, Optimization of Photovoltaic Integration

Salvatore Ardizio[1]   Fabrizio Ascione[1]   Nicola Bianco[1]   Gerardo Maria Mauro[2*]

Davide Ferdinando Napolitano[3]

1. Università degli Studi di Napoli Federico II, Department of Industrial Engineering, Piazzale Tecchio 80, 80125 Napoli, Italy
2. Università degli Studi del Sannio, Department of Engineering, Piazza Roma 21, 82100 Benevento, Italy
3. Università degli Studi di Bergamo, Via Salvecchio, 19, 24129 Bergamo, Italy

ARTICLE INFO	ABSTRACT
	This study performs the energy analysis of a real industrial building, located near Naples (South Italy). The used approach includes three phases: development of the energy model, model calibration based on monitored data and optimization of photovoltaic (PV) integration. Monitored data provide the monthly overall electricity demands of the facility for different years, while the load factors of industrial devices are not available. Thus, the assessment of hourly and daily trends of electricity demands and internal heat loads is not possible from monitored data. In order to solve such issue, the energy model of the building is developed under EnergyPlus environment, taking account of the existing PV system too. A genetic algorithm is run by coupling EnergyPlus and MATLAB® to properly calibrate the hourly load factors of the devices in order to achieve a good agreement between simulated and monitored values of monthly electricity demands. Finally, the installation of further PV panels is investigated to optimize the photovoltaic integration with a view to cost-effectiveness. The robustness of the optimization process is ensured using the calibrated energy model, which provides reliable hourly values of building electricity demand. Results show that the electricity produced by the additional PV panels is around 160 MWh per year, while the payback period is around 10 years demonstrating the financial viability of PV integration.

1. Introduction

Buildings are responsible for about 36% of total world energy consumption and for about 40% of CO_2-equivalent emissions[1]. At EU level, the situation is similar[2]. For this reason, one of the main routes to follow in order to preserve the world we live in is the sustainable development of the building sector, with the aim of reducing both polluting emissions and energy

---

Corresponding Author:
Gerardo Maria Mauro,
Università degli Studi del Sannio, Department of Engineering, Piazza Roma 21, 82100 Benevento, Italy
Email: germauro@unisannio.it

consumption. As mentioned, a large share of the latter is due to building facilities, from residential to industrial ones. The optimization of building energy performance is crucial to pursue sustainability. That is why, many countries have embarked on a common path for decades, in order to reduce the environmental impact of the building sector[3][4][5][6]. For the same reason, over the last decades, there have been several studies focused on building energy modeling, calibration and optimization[7][8], using different approaches, methodologies and optimization algorithms, in particular, numerical evolutionary ones, such as genetic algorithms[9][10], particle swarm optimization[11][12], and ant colony optimization[13][14]. Indeed, evolutionary algorithms are particularly suitable for building optimization problems, since reliable whole-building performance simulation tools usually do not provide continuous and differentiable objective functions, thereby rendering the use of analytical/classical optimization methods[15][16] extremely difficult. Definitely, the robustness of the optimization procedure is strictly related to the accuracy of the developed building energy model, which should be properly calibrated – based on real data – to provide reliable outcomes[17]. Therefore, the optimization success strongly depends on the accuracy in model development and calibration. In other words, modeling (and thus simulation), calibration and optimization are fundamental inter-dependent aspects when addressing building energy performance[18].

In 2005, Wright & Alajmi (2005) investigated the robustness of a genetic algorithm (GA) search method in solving an unconstrained building optimization problem[19], concluding that it is possible to find near-optimum solutions with a competitive (low) number of building performance simulations. In 2011, Banos et al., proposed a review of the state of the art in matter of computational optimization methods applied to renewable and sustainable energy systems[20], showing that the number of research papers using optimization methods to solve renewable energy problems had increased dramatically in recent years. The study concluded that the use of heuristic approaches, Pareto-based multi-objective optimization and parallel processing are promising research areas in the field of renewable and sustainable energy. In 2012, Heo et al. focused on the calibration of building energy models[21]. They introduced a probabilistic methodology – based on Bayesian calibration – supporting large scale investments in buildings' energy retrofit. This methodology permits to assess the risks associated with each of the retrofit options considered. In 2015, Ascione et al. proposed a new methodology for cost-optimal analysis by means of the multi-objective optimization of building energy

performance[22]. The optimization procedure was based on the coupling between MATLAB®[23] and EnergyPlus[24] by implementing a GA and supported the evaluation of profitable and feasible packages of energy efficiency measures applied to buildings. Thermal comfort was also taken into account as constraint and, finally, a ranking of the retrofit measures based on the intervention priority was estimated by identifying the most cost-effective and energy-efficient measures. In 2016, Royapoor and Roskilly performed the calibration of a 5-storey office building EnergyPlus model using energy and environmental data, collected through environmental sensors and a weather station[25]. According to the American Society of Heating, Refrigerating, and Air-conditioning Engineers (ASHRAE) guideline 14-2014[26], the model was calibrated to achieve Mean Bias Error (MBE) values within ± 5% and Cumulative Variation of Root Mean Square Error (CV(RMSE)) values below 10%. In the same vein, in 2017, Hong et al. carried out the calibration of a building energy model by using an optimization algorithm to minimize the CV(RMSE), set as objective function[27]. A similar approach was used by Lara et al., who compared the results obtained through the brute-force approach and an evolutionary optimization method adopted with the aim to calibrate an educational building model located in the North of Italy[28]. In 2017, Fan and Xia implemented a multi-objective optimization model for energy-efficiency building envelope retrofit with rooftop photovoltaic systems[29]. The optimal solutions were characterized as concerns economic indicators too, e.g., net present value and payback period, in order to support the decision-makers. In the same year, Cacabelos et al. proposed a novel building calibration approach, which consisted into dividing the building into several sub-models and calibrating them separately[30]. The results of the multi-stage calibration showed really good agreement as for energy consumption and temperature trends with lower values of MBE and CV(RMSE) on both hourly and monthly basis compared to standard calibration methodologies. Very recently, in 2019, Gao et al. investigated the different levels of data transformation between building information modeling (BIM) and building energy simulation process, including geometry (step 1), material (step 2), space type (step 3), thermal zone (step 4), space load (step 5), and HVAC system (step 6)[31]. The accuracy in data transformation is fundamental in achieving a reliable building energy model using the increasingly widespread BIM platforms. In recent times, the efforts for improving building energy efficiency are often focusing on renewable energy source systems, especially solar ones, given the high cost-effectiveness that such technologies ensure compared to the past. In 2019, Venkateswari and

Sreejith presented a comprehensive review on the factors affecting the efficiency of a solar photovoltaic (PV) cell, focusing on employed materials, maximum power point tracking (MPPT) techniques and devices used for DC-AC conversion[32]. In this regard, silicon is widely used as cell material because of its abundant availability and low cost. However, several promising multi-junction solar cell technologies ensure significantly higher values of energy efficiency and good economic indicators. Al-Addous et al. investigated the influence of weather conditions on PV power production and proposed reliable experimentally derived models to assess PV actual efficiency as a function of different temperature and radiation[33]. In addition, El Baz et al. focused on the development of a model that was capable to accurately assess the output power of a PV system according to the weather forecasts[34]. Van der Meer et al. studied the probabilistic forecasting of a residential PV power generation by means of the application of Gaussanian Processes[35]. Camilo et al. investigated the economic profitability of different PV system configuriations and concluded that storage systems are not a profitable solution, because the investments required are too high, despite the cost reduction produced, thus, the injection of the surplus into the grid is more convenient[36].

To this background, the proposed study concerns energy modeling, calibration and optimization through a comprehensive approach, which addresses a real industrial building located near Naples (South Italy). The aim is to develop a reliable building energy model in order to perform a robust optimization of photovoltaic integration. The methodology used includes three phases, as detailed in the following section: development of the energy model, model calibration based on monitored data and optimization of photovoltaic integration.

2. Methodology

The methodology used includes the following three phases:

I. Development of the energy model of the investigated industrial building, including all devices used for industrial processes;

II. Model calibration by means of the implementation of a genetic algorithm and the comparison of simulated data with real monitored data;

III. Optimization of the photovoltaic integration with the aim of minimizing global costs.

2.1 Energy Model Development

Firstly, the well-known graphical interface Design-Builder is used in order to realize the geometrical model of the industrial building and its subdivision into thermal zones[37]. It is fundamental to properly define the stratigraphy of the different elements constituting the envelope of the building, because they strongly affect the heating and the cooling demand.

Consequently, the dynamic energy simulator Energy-Plus is used for the development of the energy model of the building, since it ensures high accuracy and detail in modelling[24]. Great attention should be paid to the definition of:

1. the usage profiles for each thermal zone – i.e., the hourly schedules of occupation, people activity, clothing resistance, and so on;

2. the typology and the availability of the HVAC system;

3. the typology of the photovoltaic generator and its size.

Once the building model has been defined, EnergyPlus is used to run simulations. In order to do so, it is important to properly set the main boundary conditions of the simulations. These latter are described as per follows:

• Conduction Transfer Functions as heat balance algorithm;

• six timestep per hour;

• 20 maximum iterations for the HVAC system.

Finally, to run the dynamic energy simulations proper climatic data are necessary. The ones used are those of the authoritative ASHRAE IWEC[38] and are encoded in a proper ".epw" weather file, available at the EnergyPlus online database[39].

2.2 Energy Model Calibration

The model calibration is fundamental to achieving the schedules related to industrial devices' operation and load factors over a typical year. The accurate modeling of such devices is fundamental to obtaining reliable outcomes from simulations because the devices strongly affect building electricity consumption and internal heat loads, and thus cooling demand. In this regard, energy models of buildings can be very complex and contain a large number of input data. The accuracy of an energy model, especially when it comes to calibration, depends on the user's ability and experience in defining the input data. These parameters must, in fact, lead to a model whose energy performance reflects as closely as possible to the measured energy performance of the existing building being calibrated. The high number of input data that are required for the definition of a detailed thermal energy model makes the calibration a problem with an undefined number of solutions. The most typical approach used in the calibration of a model is the empirical one, based on the modification of the parameters "by trial and error" based on experience[40].

The steps of a correct calibration can be delineated as follows:

• Step 1: Develop an initial model of the investigated system with input data based on experience, expertise and consistency with the real system;

• Step 2: Perform an iterative procedure to improve the developed model in order to minimize error indicators, denoted as calibration indices, achieved by comparing the model outputs with real data or outputs provided by another validated (and thus reliable) model. This iterative procedure can be carried out "by trial and error" or by using optimization algorithms. In this latter case, the objective function to be minimized is provided by the mentioned error indicators. The proposed methodology uses a genetic algorithm for this purpose.

• Step 3: When a stop criterion is satisfied the iterative procedure stops and the calibrated model is achieved.

The mentioned calibration indices (i.e., error indicators) are generally achieved by comparing outputs related to energy consumption, because the real values are generally known from the building bills. For example, Pan et al. used data on electricity consumption from the sub-meter to calibrate the internal loads of the energy model of a high-rise commercial building in Shanghai[41]. Therefore, calibration methodologies generally consider monthly data related to electricity consumption to assess the error indicators of the developed model. This information is generally available for most buildings, though not all. Concerning the used metrics for calibration indices, the proposed methodology refers to ASHRAE Guideline 14-2014[26] by assessing the Mean Bias Error () and the Coefficient of Variation of Root Mean Square Error (), which are defined by equations (1) and (2), respectively:

$$MBE = \frac{1}{m}\sum_{i=1}^{m}\frac{(I_i - y_i)}{y_i} \quad (1)$$

$$CV(RMSE) = \frac{\sqrt{m\sum_{i=1}^{m}(I_i - y_i)^2}}{\sum_{i=1}^{m}y_i} \quad (2)$$

where:

• I_i is the simulated energy consumption of the ith month;

• y_i is the measured energy consumption of the ith month;

• m is the number of months, set equal to 12 because a whole year is considered.

According to ASHRAE Guideline 14[26], when the absolute values of the MBE and the CV(RMSE) are smaller than 5% and 15% respectively, the model can be considered to be well-calibrated.

As mentioned, the iterative improvement of the energy model is performed by running a genetic algorithm (GA), as shown in Figure 1. The aim is to calibrate the schedules related to industrial devices' operation and load factors. The objective function (*F*) to be minimized is the abso-

lute difference (*dEE*) between the simulated electricity consumption and the real monitored one (*F=dEE*). The decision variables are provided by the hourly load factors of industrial devices during a typical working day. They are encoded by the vector of bits $\underline{x}$. The GA stops when it is achieved a maximum number of generations (g_{max}), i.e., iterations. After that, the MBE and the CV(RMSE) are assessed according to equations (1) and (2), because the model can be considered calibrated if these values are lower than 5% and 15%, respectively.

The GA conducts a smart search within the solution domain, since it permits to investigate only a limited number of solutions, which are chosen by the optimization engine. In particular, the evolution, i.e., improvement, of a population of individuals (i.e., solutions) is performed, through successive generations (i.e., iterations) according to the processes of selection, mutation and crossover[42][43]. The logic improvement is the minimization of the objective function. The GA allows to strongly reduce the computational effort compared to an exhaustive search or a "trial and error" procedure. In this study, most GA parameters take the same values employed by Ascione et al in 2016 and 2017[42][43]. Regarding the population size s and the number of generations , they should be properly set, as the reliability of the results and the computational time are crucially affected by them. Ascione et al. assessed that reliable s values are included in the range 2-6 times the number of decision variables[42] – in this study, it is set equal to 4 – whilst reliable values are 10-100 generations – in this study, it is set equal to 30.
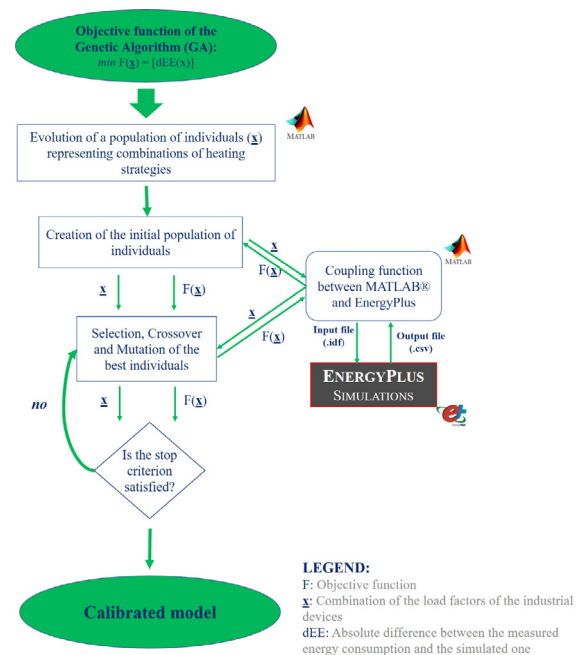

Figure 1. Flowchart of the Genetic Algorithm Implemented for Model Calibration

2.3 Optimization of Photovoltaic Integration

In this phase, the optimization of the photovoltaic (PV) integration is performed by considering the existing PV system, installed on the building roof. The energy model calibration, performed in the previous phase, is essential in order to achieve a robust optimization.

Initially, the existing photovoltaic system is accurately modeled under EnergyPlus environment, in order to have a simulated PV electricity production as close as possible to actual monitored data.

Then the PV integration is optimized in order to achieve cost-optimality, i.e., the minimization of global costs.

The Global Cost (GC) of a durable good is composed by the purchase cost, by all the necessary expenses supported for its use during its useful life, as well as by the residual value that the good possesses at the end of its useful life. The assessment of the global cost aims in assisting decision makers in choices regarding the opportunity to invest in the process building, considering the phases of conception, construction, building management. The useful life of a building can be divided into three main phases:

• *Initial phase:* from programming the intervention up to his realization;

• *Intermediate phase:* phase of occupation and management of the building;

• *Final phase:* demolition or sale of the property.

The structure of the global cost is also closely connected to these three phases, as stated by the European Union guidelines[4][44]:

$$GC = AF * RC + IC - IN - RV \quad (3)$$

where:

• *AF* is the annuity factor. It is used to calculate the present value of any future cash flow until the year "n", taking into account the discount rate "a" – usually, set equal to 3%[4][44]. Furthermore, the AF is assessed by the following equation (4):

$$AF = \frac{1}{a}\left(1 - \frac{1}{(1+a)^n}\right) \quad (4)$$

• *RC* is the annual running cost;

• *IC* is the initial cost. It is the fund needed to start up the "business";

• *IN* is the incentive that usually the Governments give to the stakeholders in order to make certain "businesses" more affordable. In this case it was assumed equal to 0;

• *RV* is the residual value. It is the value after deprecia-

tion, which is the book value of the asset. This value, in this study, was assumed equal to 0 for precautionary reasons, because RV is calculated from now to 20 years and for this reason it is close to 0.

Another critical element in the calculation of the global cost is represented by the *useful life (n)* of the building. Usually, differential useful lives are considered depending on the different building types, the different technological subsystems or the subject performing the analysis. In this study, the calculation period is assumed equal to 20 years as recommended for non-residential buildings by EU guidelines[4][44].

For a complete analysis of the investment regarding the enhancement of the photovoltaic system, besides global cost savings, further meaningful financial indices are assessed to support the decision maker: SPB, DPB and NPV.

The *simple payback period (SPB)* is the length of time required to recover the cost of an investment. It is an important determinant of whether to undertake the investment, and can be assessed according to equation (5).

$$SPB = \frac{Investment\ Cost}{Annual\ Cash\ Inflows} \quad (5)$$

The discounted payback period (DPB) is similar to the SPB, but it takes account of discounted (and not constant) cash flows, therefore it is higher than SPB and provide a more reliable metric of the investment profitably. It can be assessed according to equation (6):

$$DPB = -\frac{\log(1 - SPB * AF)}{\log(1 + AF)} \quad (6)$$

A general rule to consider when using the discounted payback period is to accept projects that have a payback period shorter than the target timeframe.

3. Description of the Case Study

The considered case study is an industrial building (Figure 2 and Table 1), a metalworking plant, located near Naples (South Italy). The gross floor area of the building is about 4800 . The glazing area represents about 5% of the floor area and about 10% of the external wall area. The plant consists of three blocks:

• the first one is divided in two floors and it is occupied by the offices and the production line;

• the second one is a one-storey block, used for the warehouse and the workshop;

• the last one was recently purchased and it is a shed that will soon be put into operation as workshop and to extend the production line.
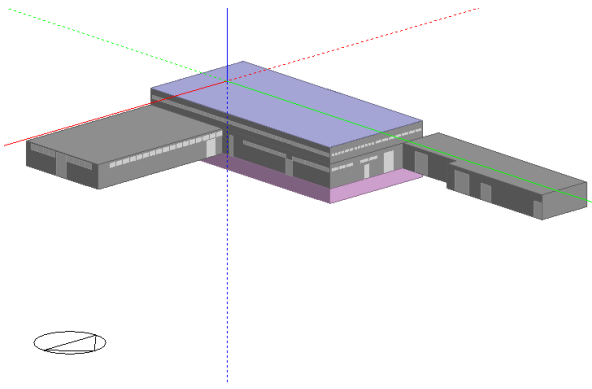
Figure 2. Rendering of the Investigated Building

Table 1. Overview About the Case Study

Case study	
Location	*District of Naples*
Category	*Industrial building*
Gross Floor Area	*4800*
Conditioned Floor Area	*1700 m²*
Levels	*2*
Level Height	*4 m*
Thermal Zones	*27*
Glazing Area	*235*

In the first block, each storey has an internal height of 4 m and are connected by a staircase. There are windows on all the facades with the aim to achieve the total building windows' surface (i.e., about 235). The geometrical model of the building has been realized with the graphical interface DesignBuilder®[37]. It has been subdivided in several thermal zones, which are different from its real subdivision in zones. In fact, a thermal zone is a part of the building that has a sufficient spatial uniformity in the temperature (and possibly in the humidity) of the air and for which there is a single and common predetermined value of the controlled variable (temperature and, possibly, set-point humidity). In addition, a thermal zone has the same type of occupation and intended use, and is served for the purpose by a single type of system, or by two complementary types. In this building, 27 thermal zones can be identified: in the first block, 10 are located at the first storey and 12 at the second one; in the storage area, there are 4 thermal zones; finally, the third block is supposed to be constituted by only one thermal zone (the shed). In order to conduct an accurate dynamic simulation, it is necessary to accurately define the geometry model and all the time-schedules concerning the end-use of each thermal zone as well as the operation parameters of the HVAC (heating, ventilation and air conditioning) systems.

The present study addresses only the first building block because the second one is characterized by very low and occasional energy consumption, while the third one has no energy consumption at all as it is an empty space, as mentioned previously.

Regarding the energy model, it is very important to consider the elements that have the highest energy consumption of the whole facility. Therefore, the consumption related to the chiller for space cooling and to the machines of the production line were assessed, other than the lights. A diesel fuel boiler is present as a heating system. However, as the main aim of this study concerns the economical convenience of a PV integration, the diesel consumption related to the heating system – which is negligible compared to the other consumption voices – is not considered. Thus, it is supposed that fan coils are used only for cooling. The building is equipped with an electric air-cooled chiller, which has a nominal coefficient of performance (COP) equal to 3.14. It is important to outline that not all the thermal zones are equipped with elements of the HVAC system.

In the firm there are 63 industrial devices, divided as follows: most devices relating to the production line are located at the groundfloor, while the rest of the devices are situated in the warehouse; these, however, are manual machines. The most extended thermal zone is the "spark erosion" one, situated at the groundfloor. As expected, as this is the biggest zone with the highest number of machines, it is, consequently, the zone with the greatest energy consumption.

4. Results and Discussion

4.1 Calibration

In order to have a reliable energy model of the building, the proper calibration of the operation of the industrial devices of the production line is fundamental. Unfortunately, there is no data on the manufacturability on a monthly basis of the devices because the facility works on commission, thus it is very difficult to establish a precise energy consumption for each device. Therefore, as explained in Methodology, a calibration process making use of the coupling between the dynamic energy simulator EnergyPlus and the optimization engine MATLAB® is used in order to evaluate the schedules of load factors for such devices. More in detail, a genetic algorithm is implemented in MATLAB® to identify the combination of load factors that month by month assures the lowest difference in terms of electricity consumption between the simulation results and real monitored data related to 2017. Table 2 compares real monitored data of the electricity consumption of industrial devices for 2017 and 2018 against simulated outputs of the calibrated model,

reflecting very good model consistency with real data.

Table 2. Electricity Consumption of Industrial Devices: Simulated Outputs of the Calibrated Model vs Real Monitored Data of 2017 and 2018

Month	Electricity demand				
	Simulated data [kWh]	Real data of 2017 [kWh]	Discrepancy: Simulated vs Real 2017	Real data of 2018 [kWh]	Discrepancy: Simulated vs Real 2018
January	112'352	112'303	0.044%	120'406	-6.69%
February	103'794	103'723	0.068%	109'731	-5.41%
March	106'449	106'349	0.094%	121'411	-12.32%
April	105'016	104'915	0.096%	117'637	-10.73%
May	116'824	116'745	0.068%	132'896	-12.09%
June	126'866	126'819	0.037%	134'868	-5.93%
July	134'076	133'994	0.061%	147'477	-9.09%
August	121'603	121'576	0.022%	113'676	6.97%
September	116'511	116'487	0.021%	124'731	-6.59%
October	113'744	113'736	0.007%	119'956	-5.18%
November	113'008	112'894	0.101%	114'147	-1.00%
December	117'962	118'016	-0.046%	119'822	-1.55%
Total	1'388'205	1'387'557	0.047%	1'476'758	-6.00%

Table 2 shows the measured values of electricity consumed by the facility, around 100 MWh per month, and compares them with the result of EnergyPlus simulation making use of the optimal combination of load factors for the industrial devices. Differences are very low, especially for 2017, which means that the model has been properly calibrated.

Overall, in 2017, the electricity required is around 1'388 MWh. The non-linearity of the electricity demand, which is due to the fact that the firm does not work in series but works on commission, leads to a non-linearity of the energy values required month by month. In fact, the devices of the production line do not work every day, every hour and with the same work shifts, but there are variations of processing day by day depending on the requests. As mentioned, the load factors of each machine are obtained by means of an optimization process making use of a genetic algorithm, which provides the processing coefficient of each device. The load factors of each device are very low. In fact, they are generally equal to 0.30 or 0.40, and in some cases, they are 0.00. In few cases, peaks of 0.80 or 0.90 are reached. This is due to the main feature of the company that works on commission, therefore this does

not allow to have a calibration linearity. Furthermore, each process requires an alternate use of several devices, which is why the load coefficients are often low, since a single product to be processed is subject to a machining chain (eg, turning, milling, erosion, etc.).

The results of the simulation are compared with the measured data for 2018 too, in order to evaluate the goodness and the robustness of the calibration. Table 2 shows that electricity consumption has slightly increased compared to the previous year, probably due to a change in processing fees and the implementation of new processing industrial devices. In fact, in 2018 it is noted that on average the monthly values settle around 110/120 MWh and a total of 1'477 MWh per year. It is possible to note an increase of around 10% compared to the previous year. This involves a greater variation than the simulated values even if they are always very low percentages around 3-4%. Here, too, it can be noted, for example, that in July the demand for electricity is around 148 MWh, while for other months it is around 30 MWh less, demonstrating that the industrial devices do not work linearly month by month but are dependent on customer requests.

4.2 Photovoltaic Integration

On the main surface of the first block, the facility presents a photovoltaic system on a surface of approximately 1710 . This photovoltaic system has a peak power of 224.64 kWp and is connected to the electricity grid, Enel, in medium voltage (MT). The plant is made of monocrystalline silicon panels with peak power of 150 W per panel, maximum power point voltage of 18.5 V, maximum power point current intensity of 8.62 A, open circuit voltage of 22.75 V, short circuit current intensity of 8.62 A, module efficiency of 15%, panel surface around 1 m^2.

The roof on which the system is built is flat and for the installation of the modules an inclined structure of 5° (Tilt) has been built and oriented to the south to optimize the production of the plant itself. The modules are firmly anchored to aluminum structures attached to concrete supports resting on the roof. The PV generator consists of 864 photovoltaic modules, eight string inverters each of which has two independent MPPT (Maximum Power Point Trackers). Three strings are connected to each MPPT of each inverter and each string is composed of 18 modules connected in series.

The existing PV system produced around 305 MWh in 2017 and 285 MWh in 2018, and this electricity was self-consumed with 0% injected into the network. Table 3 shows the electricity production of the existing photovoltaic plant by comparing simulated outputs against real monitored data of 2017 and 2018.

Table 3. Electricity Production of the Existing Photovoltaic Plant: Simulated Outputs vs Real Monitored Data of 2017 and 2018

Month	Electricity production of existing Photovoltaics				
	Simulated data [kWh]	Real data of 2017 [kWh]	Discrepancy: Simulated vs Real 2017	Real data of 2018 [kWh]	Discrepancy: Simulated vs Real 2018
January	10'865	11'758	7.59%	10'758	0.99%
February	14'498	12'544	15.58%	10'411	39.26%
March	23'076	21'205	8.82%	19'400	18.95%
April	28'663	32'224	-11.05%	31'669	-9.49%
May	38'582	39'547	-2.44%	33'600	14.83%
June	38'057	40'833	-6.80%	38'700	-1.66%
July	40'578	41'211	-1.54%	39'678	2.27%
August	36'084	37'026	-2.54%	32'076	12.50%
September	26'307	27'667	-4.92%	28'089	-6.34%
October	19'409	22'894	-15.22%	18'854	2.94%
November	11'888	11'937	-0.41%	11'667	1.89%
December	9'640	7'907	21.92%	9'723	-0.85%
Total	294'920	306'753	-3.86%	284'625	3.62%

The electricity production of the PV system depends on some factors, which can explain the difference between years 2017 and 2018:

• the sun radiation is clearly the main factor affecting electricity production and it is not the same for all years;

• the temperature makes the difference and affects the yield. The optimal temperature is generally estimated at around 25 °C. In this case the classic photovoltaic panel has the best conditions to produce energy. Excessive overheating or an insufficient level of ventilation causes a proportional decrease in production;

• the presence of dust and dirt on the modules hinders the full receptivity of the solar irradiation on the photovoltaic cells;

• the passage, or worse the constant presence, of shadows during the day. A typical example is the shade of chimneys, antennas or trees that can cover part of the panels during the day, hindering the efficiency of the entire system.

During the summer months, the production of the PV system is higher than winter months because the days present more hours of sun. It is possible to see that there is a low difference between the values related to the measured production and to the simulated one. The

percentage absolute difference (%) is around 3-4% for both 2017 and 2018. The simulated value of PV electricity production, as shown in Table 3, is placed right in the middle between the data of 2017 and 2018.

The electricity production of the existing PV system is lower than facility electricity demand, given the high values of energy demands by industrial devices and space cooling equipment. Thus, the study addressed the optimization of a further PV integration with a view to cost-optimality. Indeed, the enhancement of the PV system can be highly cost-effective given the huge values of facility electricity consumption.

The new PV panels have the same characteristics of existing ones and are installed on the building roof with the same orientation and tilt angle. Different sizes are considered in terms of coverage of the non-occupied roof surface (around 830 m^2) by photovoltaics, set equal to:

• around 25% coverage of roof area, corresponding to 210 panels and to a peak power of 31.5 kWp;

• around 50% coverage roof area, corresponding to 400 panels and to a peak power of 60 kWp;

• around 75%, corresponding to 600 panels and to a peak power of 90 kWp;

• around 100%, corresponding to 825 panels and to a peak power of 123.75 kWp.

The panel numbers have been chosen in order to ensure complete strings. The financial benefits of PV integration are assessed in terms of global cost reduction. In order to investigate the sensitivity to investment cost variation, two values are considered for PV purchase cost, i.e., 1200 €/kWp (case A) and 1700 €/kWp (case B), respectively, according to current market prices.

For example, Figure 3 shows the PV productions of both the existing PV system and the integrated one, which takes into account the cover of 100% of the roof area.
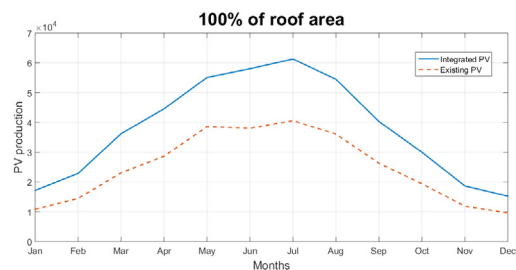

Figure 3. Monthly Electricity Production of PV Panels Covering the 100% of the Non-occupied Roof Area

The performance of PV integration covering the different percentage of the roof area considered in Tables 4, 5, 6 and 7 – i.e., 25%, 50%, 75% and 100%, respectively – by reporting:

• the electricity production of existing PV systems;

• the electricity production of PV integration;

- total electricity production of PV;
- electricity sold to the grid.

The electricity production of existing PV system is reported in each of the following summentioned tables, in order to make any comparison clearer for the readers.

Table 4. Production of PV Panels Covering the 25% of the Non-occupied Roof Area

Month	Electricity production of existing PV [kWh]	Electricity production of PV integration [kWh]	Total Electricity production of PV [kWh]	Electricity sold to the grid [kWh]
January	10'865	1'613	12'478	0
February	14'498	2'133	16'631	106
March	23'076	3'342	26'418	164
April	28'663	4'048	32'711	780
May	38'582	4'891	43'743	2'137
June	38'057	5'083	43'140	3'199
July	40'578	5'271	45'849	1'120
August	36'084	4'680	40'764	1'477
September	26'307	3'562	29'869	293
October	19'409	2'697	22'106	64
November	11'888	1'731	13'619	0
December	9'640	1'431	11'071	0
Total	294'920	40'482	335'402	9'340

Table 5. Production of PV Panels Covering the 50% of the Non-occupied Roof Area

Month	Electricity production of existing PV [kWh]	Electricity production of PV integration [kWh]	Total Electricity production of PV [kWh]	Electricity sold to the grid [kWh]
January	10'865	3'072	13'937	0
February	14'498	4'062	18'560	240
March	23'076	6'365	29'441	445
April	28'663	7'710	36'373	1'386
May	35'852	6'586	45'168	3'388
June	38'057	9'681	47'738	4'479
July	40'578	10'039	50'617	2'128
August	36'084	8'915	44'999	2'475
September	26'307	6'785	33'092	752
October	19'409	5'137	24'546	239
November	11'888	3'297	15'185	0
December	9'639	2'724	12'364	0
Total	294'916	74'373	369'293	15'633

Table 6. Production of PV Panels Covering the 75% of the Non-occupied Roof Area

Month	Electricity production of existing PV [kWh]	Electricity production of PV integration [kWh]	Total Electricity production of PV [kWh]	Electricity sold to the grid [kWh]
January	10'865	4'608	15'473	0
February	14'498	6'092	20'590	563
March	23'076	9'548	32'624	1'041
April	28'663	11'565	40'228	2'319
May	38'582	11'244	49'826	5'136
June	38'057	14'521	52'578	6'379
July	40'578	15'059	55'637	3'236
August	36'084	13'372	49'456	3'548
September	26'307	10'178	36'485	1'377
October	19'409	7'705	27'114	559
November	11'888	4'946	16'834	4.1
December	9'640	4'086	13'726	0
Total	294'920	112'924	407'844	24'162

Table 7. Production of PV Panels Covering the 100% of the Non-occupied Roof Area

Month	Electricity production of existing PV [kWh]	Electricity production of PV integration [kWh]	Total Electricity production of PV [kWh]	Electricity sold to the grid [kWh]
January	10'865	6'335	17'200	5
February	14'498	8'377	22'875	1'139
March	23'076	13'129	36'205	2'017
April	28'663	15'903	44'566	3'728
May	38'582	16'485	55'067	7'456
June	38'057	19'967	58'024	8'819
July	40'578	20'706	61'284	4'539
August	36'084	18'387	54'471	4'796
September	26'307	13'995	40'302	2'296
October	19'409	10'594	30'003	1'111
November	11'888	6'801	18'689	39
December	9'640	5'618	15'258	0
Total	294'920	160'297	455'217	35'944

Concerning the 25% PV coverage, the electricity production increases of around 40 MWh per year and the sold electricity is around 9 MWh per year. Considering the existing PV system, the production capacity complexively rises to 335 MWh per year. During warm months, the integration system guarantees an electricity production between 4-5 MWh per month, while during the rest of the year its production is between 0 and around 3 MWh per month. Finally, the sold energy is equal to 2-3 MWh per month in warm periods, while it assumes values included between 0 and 1 MWh per month for the rest of the year.

When the PV integration covers the 50% of roof area, the electricity production increases of around 74 MWh per year and the sold electricity is around 16 MWh per year. Overall, a production of 369 MWh per year is achieved. Considering exclusively the PV integration system, this latter produces around 9-10 MWh per month during the warmer period, while its production is included between 3 and 7 MWh per month for the rest of the year, with the exception of April, when the electricity production has a peak equal to around 8 MWh. Concerning the sold energy, it is possible to observe that it reaches about 3-4 MWh per month in the warm months and values between 0 and 2 MWh per month in the other months.

Concerning the 75% PV coverage, the electricity production increases of around 113 MWh per year and the sold electricity is around 24 MWh per year. Considering the existing PV system, the production capacity complexively rises to 408 MWh per year. During warm months, the integration system permits to produce around 15 MWh per month. Finally, the sold energy is equal to 5-6 MWh per month in the warm period, while it assumes values included between 0 and 3 MWh per month for the rest of the year.

In conclusion, when the PV integration covers the 100% of roof area, the electricity production increases of around 160 MWh per year and the sold electricity is around 36 MWh per year. In this case, a total production capacity of 455 MWh per year is achieved, reaching with the second plant about 20 MWh per month in the warm months and 6-16 MWh per month during the rest of the year. The sold energy is equal to 7-8 MWh per month during the warmer period, while it is included between 0 and 4 MWh per month for the rest of the year. Finally, such PV integration can reduce (to close to zero) the electricity taken from the grid by supporting the facility self-sustainability.

Table 8 shows the cost/financial analysis of the proposed solutions by reporting the global cost saving compared to the baseline for cases A (panel purchase cost of 1200 €/kWp) and B (panel purchase cost of 1700 €/kWp).

It is clear, for both scenarios, the cost-optimal solution is the 100% PV integration, which can yield a global cost saving between 134 k€ (case A) and 70 k€ (case B) during the facility lifespan, with simple payback (SPB) between 7.3 and 10.4 years, discounted payback (DPB) between 8.4 and 12.7 years.

Table 8. Cost Analysis of New PV Panels

Roof covering	Global Cost Saving for Case A	Global Cost Saving for Case B
100%	133.840 k€	69.837 k€
75%	97.252 k€	51.252 k€
50%	67.199 k€	35.699 k€
25%	32.783 k€	23.778 k€

5. Limitations and Further Developments

Despite the effectiveness of the calibration method, and the robustness of the results, which was confirmed by the comparison with the measured data related to the year 2018 too, the study here proposed presents a limit.

The lack of data related to on-site measurements concerning the energy consumption of each device and to the local weather conditions has obliged the authors to make some simplifications, in order to calibrate the energy model and investigate the cost-effectiveness of the PV integration for the firm. In usual conditions, the normalization of the bill consumptions would have been required as well as the use of on-site monitored weather data. However, the latter were unavailable, especially the productivity of each device, due to the fact that the company works on commission. For this reason, the only way to proceed was to calibrate the energy model based on typical weather conditions and by considering the energy consumptions reported on the bills. This operation was performed referring to the energy bills of the year 2017. As verification, the monthly energy consumption values assessed by the model were compared with the ones monitored the following year 2018. Being the main calibration indexes limit values – evaluated on the yearly global energy performance – respected also for this different year, the model was considered "calibrated". This approach was adopted also for modelling and calibrating the existing PV system.

The unavailability of data concerning the piece production of each device, and in turn, their individual electricity consumption, has obliged the authors to use the genetic algorithm, in order to estimate the load factors of each device. However, the assessed load factors could be different from the real one – if measured –, even if the global electricity consumption of the production site resulting from the energy simulations is approximately the same of the measured one. As further development, it would be interesting to measure on site the load factors of the devices, if

possible, and, consequently, re-calibrate the energy model. In fact, with the re-calibrated model, it would be possible to investigate also the thermal comfort of the workers, because it would be known the exactly disposition of the internal gain sources, and so it would be also possible to optimize the operation of the HVAC (heating, ventilation and air conditioning) system, considering the thermal comfort and the running costs as objective functions.

In addition, another interesting improvement that could be done to the energy model is the calibration of the CO_2 emissions and, more in general, of the environmental impact – from the energy point of view. Once done, a genetic algorithm could be performed, in order to evaluate the optimal energy retrofit strategy for the firm, considering the cost-effectiveness and the environmental sustainability as main targets.

6. Conclusion

The study investigated the energy performance of an industrial building. The facility energy model was developed under EnergyPlus environment by considering all industrial devices, which deeply affect electricity consumptions and cooling needs. Since the operation and load schedules of the devices were not available, an accurate calibration procedure was performed based on the implementation of an optimization genetic algorithm and on the comparison between simulated data and real monitored data concerning electricity consumption. The calibration procedure provided optimal results because the calibrated model presented very low values of the calibration coefficients, i.e., error indicators, suggested by ASHRAE guideline 14-2014. Indeed, the MBE (mean bias error) was around 0.05% and the Coefficient of Variation of Root Mean Square Error (CV(RMSE)) was around 0.20%, whereas the limit values recommended by ASHRAE to have a calibrated model are 5% and 15%, respectively.

After the model calibration, the integration of the existing photovoltaic (PV) system is investigated in order to achieve cost-optimality. Indeed, the facility is characterized by the huge electric loads, given the industrial devices, and the existing PV system can be enhanced with high financial benefits. The study showed that the cost-optimal measures is the installation of a full-roof PV system, since this provide global cost savings I 20 years between 70 and 134 k€ (depending on the purchase cost) with payback times around 10 years.

Generally speaking, even if the results could appear quite obvious, it is important to remark that an accurate model calibration is always fundamental to achieve robust optimization results. In fact, having a well-calibrated energy model, even other energy retrofit measures concerning the power system could have been easily taken into account, in order to reduce the environmental impact of the building. This could be another interesting point to investigate further.

References

[1] Energy Efficiency. Retrieved September 5, 2019, from https://www.iea.org/topics/energyefficiency/buildings/.

[2] Energy performance of buildings - European Commission. Retrieved August 29, 2019, from https://ec.europa.eu/energy/en/topics/energy-efficiency/buildings.

[3] EU Commission and Parliament. Directive 2002/91/EC of the European Parliament and of the Council of 16 December 2002 on the Energy Performance of Buildings (EPBD). Retrieved September 4, 2019, from https://eur-lex.europa.eu/legal-content/EN/TXT/?uri=celex%3A32002L0091.

[4] EU Commission and Parliament. Directive 2010/31/EU of the European Parliament and of the Council of 19 May 2010 on the Energy Performance of Buildings (EPBD Recast). Retrieved September 4, 2019, from http://www.buildup.eu/en/practices/publications/directive-201031eu-energy-performance-buildings-recast-19-may-2010 (last accessed on 09/04/2019).

[5] European Parliament and the Council Directive 2018/844/EU of 30 May 2018 amending Directive 2010/31/EU on the energy performance of buildings and Directive 2012/27/EU on energy efficiency. Retrieved September 4, 2019 from https://eur-lex.europa.eu/legal-content/EN/TXT/PDF/?uri=CELEX:32018L0844&from=EN

[6] The Paris Agreement. Retrieved September 5, 2019, from https://unfccc.int/process-and-meetings/the-paris-agreement/the-paris-agreement.

[7] Attia S., Carlucci S., Hamdy M., O'Brien W. (2013). Assessing gaps and needs for integrating building performance optimization tools in net zero energy buildings design. Energy and Buildings, 60, 110-24.

[8] Kheiri, F. (2018). A review on optimization methods applied in energy-efficient building geometry and envelope design. Renewable and Sustainable Energy Reviews, 92, 897-920.

[9] Yu, W., Li, B., Jia, H., Zhang, M., & Wang, D. (2015). Application of multi-objective genetic algorithm to optimize energy efficiency and thermal comfort in building design. Energy and Buildings, 88, 135-143.

[10] Ruiz, G. R., Bandera, C. F., Temes, T. G. A., & Gutierrez, A. S. O. (2016). Genetic algorithm for building envelope calibration. Applied Energy, 168, 691-705.

[11] Xuemei, L., Ming, S., Lixing, D., Gang, X., & Jibin,

L. (2010). Particle swarm optimization-based LS-SVM for building cooling load prediction. Journal of Computers, 5(4), 614-621.

[12] Delgarm, N., Sajadi, B., Kowsary, F., & Delgarm, S. (2016). Multi-objective optimization of the building energy performance: A simulation-based approach by means of particle swarm optimization (PSO). Applied energy, 170, 293-303.

[13] Bamdad, K., Cholette, M. E., Guan, L., & Bell, J. (2017). Building Energy Optimisation Using Artificial Neural Network and Ant Colony Optimisation. In AIRAH and IBPSA's Australasian Building Simulation 2017 Conference, Melbourne.

[14] Bamdad, K., Cholette, M. E., Guan, L., & Bell, J. (2017). Ant colony algorithm for building energy optimisation problems and comparison with benchmark algorithms. Energy and Buildings, 154, 404-414.

[15] Nguyen, A. T., Reiter, S., Rigo, P. (2014). A review on simulation-based optimization methods applied to building performance analysis. Applied Energy, 113, 1043-58.

[16] De Boeck, L., Verbeke, S., Audenaert, A., & De Mesmaeker, L. (2015). Improving the energy performance of residential buildings: A literature review. Renewable and Sustainable Energy Reviews, 52, 960-975.

[17] Asadi, S., Mostavi, E., Boussaa, D., & Indaganti, M. (2019). Building Energy Model Calibration Using Automated Optimization-Based Algorithm. Energy and Buildings.

[18] Ahmad, M., & Culp, C. H. (2006). Uncalibrated building energy simulation modeling results. HVAC&R Research, 12(4), 1141-1155.

[19] Wright, J., Alajmi, A. (2005, August). The robustness of genetic algorithms in solving unconstrained building optimization problems. In Proceedings of the 7th IBPSA Conference: Building Simulation, Montréal, Canada August (pp. 15-18).

[20] Banos, R., Manzano-Agugliaro, F., Montoya, F. G., Gil, C., Alcayde, A., Gómez, J. (2011). Optimization methods applied to renewable and sustainable energy: A review. Renewable and sustainable energy reviews, 15(4), 1753-66.

[21] Heo, Y., Choudhary, R., Augenbroe, G. A. (2012). Calibration of building energy models for retrofit analysis under uncertainty. Energy and Buildings, 47, 550-60.

[22] Ascione, F., Bianco, N., De Stasio, C., Mauro, G. M., Vanoli, G. P. (2015). A new methodology for cost-optimal analysis by means of the multi-objective optimization of building energy performance. Energy

and Buildings, 88, 78-90.

[23] MathWorks, MATLAB – MATrixLABoratory. (2015). User's Guide (version 8.5.0).

[24] Nrel. NREL/EnergyPlus. Retrieved November 27, 2018, from https://github.com/NREL/EnergyPlus/releases/tag/v8.6.0

[25] Royapoor, M., Roskilly, T. (2015). Building model calibration using energy and environmental data. Energy and Buildings, 94, 109-20.

[26] ASHRAE Guideline 14-2014. (2014). Guideline 14-2014. Measurement of energy, demand, and water savings. American Society of Heating, Refrigerating, and Air Conditioning Engineers, Atlanta, GA.

[27] Hong, T., Kim, J., Jeong, J., Lee, M., Ji, C. (2017). Automatic calibration model of a building energy simulation using optimization algorithm. Energy Procedia, 105, 3698-704.

[28] Lara, R. A., Naboni, E., Pernigotto, G., Cappelletti, F., Zhang, Y., Barzon, F., ... Romagnoni, P. (2017). Optimization tools for building energy model calibration. Energy Procedia, 111, 1060-69.

[29] Fan, Y., Xia, X. (2017). A multi-objective optimization model for energy-efficiency building envelope retrofitting plan with rooftop PV system installation and maintenance. Applied Energy, 189, 327-35.

[30] Cacabelos, A., Eguía, P., Febrero, L., Granada, E. (2017). Development of a new multi-stage building energy model calibration methodology and validation in a public library. Energy and Buildings, 146, 182-99.

[31] Gao, H., Koch, C., Wu, Y. (2019). Building information modelling based building energy modelling: A review. Applied Energy, 238, 320-43.

[32] Venkateswari, R., Sreejith, S. (2019). Factors influencing the efficiency of photovoltaic system. Renewable and Sustainable Energy Reviews, 101, 376-94.

[33] Al-Addous, M., Dalala, Z., Class, C. B., Alawneh, F., Al-Taani, H. (2017). Performance analysis of off-grid PV systems in the Jordan Valley. Renewable Energy, 113, 930-41.

[34] El-Baz, W., Tzscheutschler, P., & Wagner, U. (2018). Day-ahead probabilistic PV generation forecast for buildings energy management systems. Solar Energy, 171, 478-490.

[35] van der Meer, D. W., Shepero, M., Svensson, A., Widén, J., & Munkhammar, J. (2018). Probabilistic forecasting of electricity consumption, photovoltaic power generation and net demand of an individual building using Gaussian Processes. Applied energy, 213, 195-207.

[36] Camilo, F. M., Castro, R., Almeida, M. E., & Pires, V. F. (2017). Economic assessment of residential PV

systems with self-consumption and storage in Portugal. Solar Energy, 150, 353-362.

[37] DesignBuilder Software – V. 5.0.3.7, DesignBuilder Software Ltd, Gloucestershire, UK, 2017. Available online: www.designbuilder.co.uk (accessed on 05 04 2018).

[38] ASHRAE, 2002. American Society of Heating, Refrigerating and Air-Conditioning Engineers, ASHRAE Handbook HVAC Applications, International weather for energy calculations (IWEC Weather Files) User's Manual. U.S. Atlanta, GA 30329.

[39] Weather Data. Retrieved November 27, 2018, from https://energyplus.net/weather.

[40] Desideri, U., & Asdrubali, F. (Eds.). (2018). Handbook of Energy Efficiency in Buildings: A Life Cycle Approach. Butterworth-Heinemann.

[41] Pan, Y., Huang, Z., Wu, G. (2007). Calibrated building energy simulation and its application in a high-rise commercial building in Shanghai. Energy and Buildings, 39(6), 651-57.

[42] Ascione, F., Bianco, N., De Stasio, C., Mauro, G. M., Vanoli, G. P. (2016). Multi-stage and multi-objective optimization for energy retrofitting a developed hospital reference building: A new approach to assess cost-optimality. Applied energy, 174, 37-68.

[43] Ascione, F., Bianco, N., De Masi, R. F., Mauro, G. M., Vanoli, G. P. (2017). Resilience of robust cost-optimal energy retrofit of buildings to global warming: A multi-stage, multi-objective approach. Energy and Buildings, 153, 150-167.

[44] Commission Delegated Regulation No 244/2012. Available online: http://www.buildup.eu/sites/default/files/content/l_08120120321en00180036.pdf (accessed on 27 11 2018).